Thermal anomalies associated with forced and free ground-water convection in the Dead Sea rift valley

Haim Gvirtzman *Institute of Earth Sciences, Hebrew University of Jerusalem, Jerusalem 91904, Israel*

Grant Garven *Department of Earth and Planetary Sciences, Johns Hopkins University, Baltimore, Maryland 21218*

Gdaliahu Gvirtzman *Department of Geography, Bar Ilan University, Ramat Gan 52900, Israel*

ABSTRACT

The Dead Sea rift valley is a left-lateral transform, along which several rhomb-shaped grabens were formed. At the Sea of Galilee, which is one of these rhomb-shaped grabens, ambiguous heat fluxes were measured: 70–80 mW/m^2 at the central part of the lake, 36 mW/m^2 at the lake's southern coast (10 km apart), and most surprising, about 135 mW/m^2 at the southern Golan Heights, 6–8 km east of the graben margin. A detailed geologic cross section, traversing the entire sedimentary basin, was constructed. The hydrodynamics in this cross section were analyzed quantitatively using a two-dimensional finite element code that solves the coupled variable-density ground-water flow and conductive-convective heat transfer equations. On the basis of numerical simulations, different mechanisms of basin-scale ground-water convection are suggested for the two sides of the rift that could influence the transport of heat: (1) forced convection (gravity-driven flow) of hot brines from deeper aquifers to the land surface at the western side; and (2) large-scale free convection (buoyancy-driven flow) of deep ground water at the eastern side. The different heat fluxes within the rift valley are attributed to the different lithologies and to the locations of specific conduits through which the hot ground waters ascend from deeper horizons. These simulations also explain the different salinities of the hot springs on the two sides of the rift.

*e-mail: haimg@vms.huji.ac.il

INTRODUCTION

Deep ground-water flow plays a major role in many geologic processes (Bredehoeft and Norton, 1990). Hydrothermal ore deposits, petroleum migration and entrapment, diagenesis of sediments, and geothermal anomalies provide excellent examples of the dynamic coupling of large-scale hydrologic systems and the evolution of the Earth's crust (Bethke and Marshak, 1990; Garven et al., 1993). Sedimentary basins are subject to several forces known to cause large-scale ground-water migration, each characterized by a typical flow rate, as reviewed by Garven (1995). Gravity-driven flow resulting from a slope in the ground-water table is the most familiar mechanism and is characterized by flow rates on the order of 10 m/yr. Buoyancy-driven flow associated with temperature and salinity gradients creates free convection with flow rates of 1 m/yr at most. The above two mechanisms may be stable over a relatively long period of time, thus, steady-state flow conditions may persist. Compaction-driven and tectonically driven flows associated with abnormal overpressure, which dissipates quickly when stress relaxes induce flow rates of 0.1–0.01 m/yr.

Geothermal anomalies induced by ground-water flow involve either forced convection through open systems (gravity- or pressure-driven flow), or free convection within closed systems (buoyancy-driven flow), and in some places, both convective systems may coexist. Forced ground-water convection is a well-known phenomenon, observed at large and small basins throughout the world. It was identified either directly, on the basis of hydraulic head distribution (e.g., Toth, 1978; Habermehl, 1980), or indirectly, using geochemical (e.g., Musgrove and Banner, 1993; Bentley et al., 1986) or geothermal observations (e.g., Deming et al., 1992). Quantitative analysis of such flow systems has been applied at several basins using hydrogeological modeling (reviewed by Person et al., 1996). On the other hand, relatively less evidence exists for natural free ground-water convection. Such convection may result from several different causes: (1) thermal perturbations within the upper Earth's crust induced by intrusive igneous bodies (Norton and Knight, 1977); (2) temperature variations at mid-ocean ridges inducing sea-water circulation (Anderson et al., 1979); and (3) salinity variations of formation water in sedimentary basins at the vicinity of salt diapirs (Hanor, 1987; Evans and Nunn, 1989). In principle, when permeable, fluid-saturated, sedimentary layers are subjected to normal geo-thermal gradients (about 25 °C/km), convection cells will spontaneously arise and persist (Wood and Hewett, 1982). However, quantitative documentation of this phenomenon is rare. This paper analyzes quantitatively a unique relationship at a continental rift between both forced and free ground-water convections associated with geothermal anomalies.

The study was carried out at the Sea of Galilee region, located within the Dead Sea rift valley (Fig. 1), which includes the lowest land-surface elevations on Earth. The Dead Sea rift is a left-lateral strike-slip transform, separating the Sinai-Levant subplate from the Arabian plate. Along this transform, several en echelon rhomb-shaped grabens were formed, including the Hula basin, the Sea of Galilee, and the Dead Sea (Garfunkel, 1981). The lateral shift along this transform is estimated to be 105 km. This deep base level serves as a discharge area for a gravity-driven ground-water flow system at the western side of the graben. We suggest that large-scale free convection cells of deep ground water persist on the eastern side of the graben.

GSA Bulletin; September 1997; v. 109; no. 9; p. 1167–1176; 5 figures; 3 tables

HEAT-FLUX DATA

Through an extensive study at 70 locations in Israel (Fig. 2), a mean heat flux of 50 mW/m^2 with a standard deviation of 24 mW/m^2 was calculated (Eckstein, 1976; Eckstein and Simmons, 1978). The heat flux equals the product of thermal conductivity and temperature gradient. The thermal conductivities were determined using core samples, and temperature gradients were measured in a series of deep oil and water wells at depths of several hundreds of meters using a thermistor probe. Other workers have subsequently measured temperature gradients in additional deep wells (Levitte and Olshina, 1985; Kashai and Croker, 1987). All these studies have shown that gradients of 15–25 °C/km are common along the Dead Sea rift valley. Similarly, a U.S. Geological Survey team has measured the heat fluxes in 18 boreholes at depths of several hundreds of meters at the State of Jordan (Galanis et al., 1986). They have reported that the average heat flux is 53 mW/m^2, and it ranges between 42 and 65 mW/m^2 (Fig. 2).

The common heat fluxes at these two neighboring states, Israel and Jordan, are slightly higher than those measured at the Mediterranean Sea, and slightly lower than those at the Red Sea. Erickson et al. (1977) reported that the average heat flux at the eastern Mediterranean Sea is 31 mW/m^2 with a standard deviation of 13 mW/m^2, whereas heat fluxes in the range of 60–340 mW/m^2 were detected at the Red Sea (Erickson and Simmons, 1969) at the vicinity of a relatively young mid-ocean ridge. It seems, however, that the Dead Sea rift valley is not definitely different from its surrounding mountain chains (Ben-Avraham et al., 1978; Kashai and Croker, 1987); only at some specific spots are higher geothermal fluxes found (Eckstein and Maurath, 1995). This normal heat flux is surprising because continental rifting is thought to accompany stretching and thinning of the lithosphere, resulting in an elevated geothermal gradient (McKenzie, 1978). However, no thinning of the lithosphere is evident along the Dead Sea Transform (Folkman, 1980), and, therefore, a heat flux anomaly is not necessarily expected.

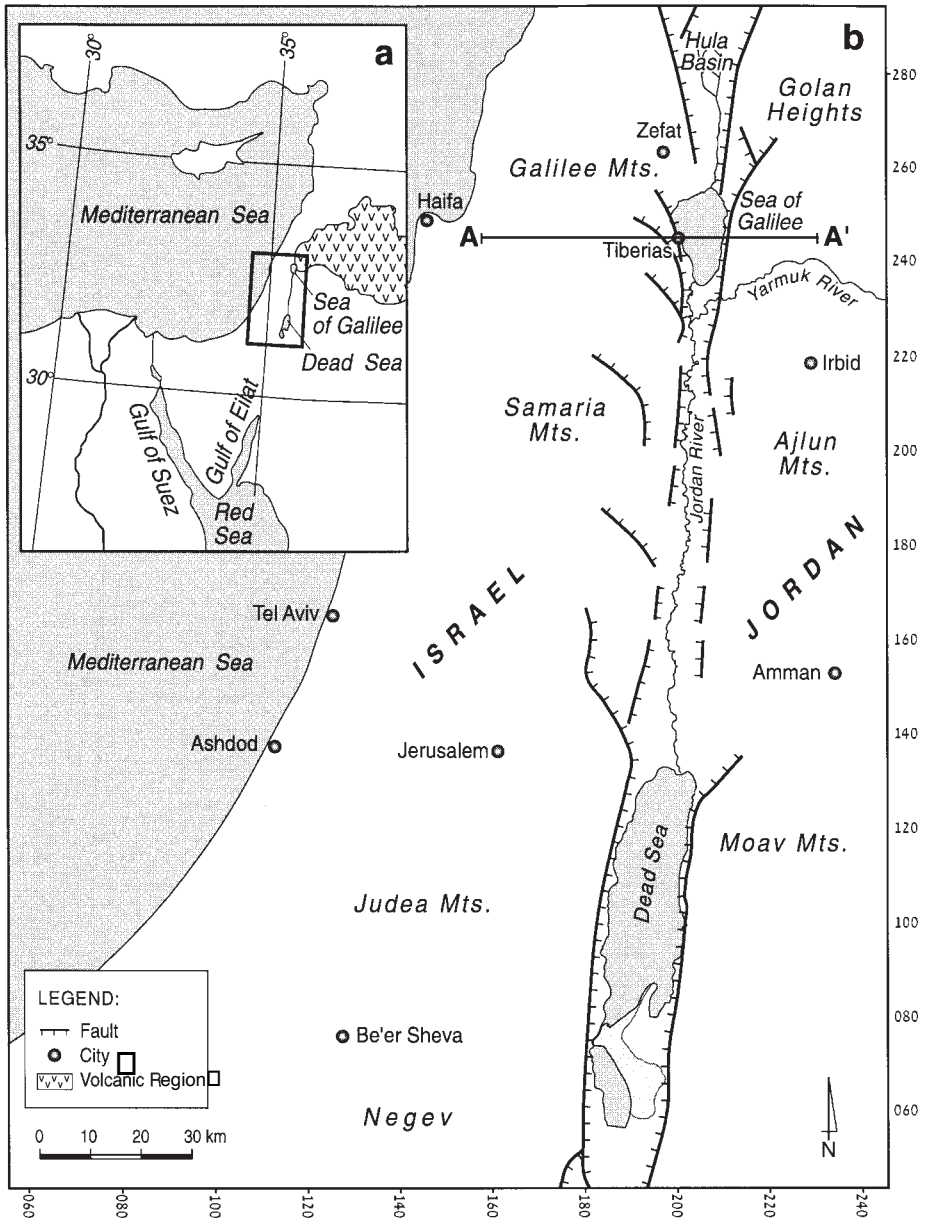

Figure 1. Location maps of (a) the studied area and its vicinity, showing the large volcanic province; and (b) the Dead Sea rift valley fault system and the mountains on both sides, in Israel and Jordan. A–A′ is a geologic cross section (Fig. 4). Map coordinates are of Israeli grid system.

It is surprising that ambiguous heat fluxes were detected at the Sea of Galilee, within the Dead Sea rift valley (Fig. 2b). Ben-Avraham et al. (1978) measured a relatively high mean heat flow of 74 mW/m^2 (range between 70 and 80 mW/m^2) in the Sea of Galilee using an outboard heat flow probe. Temperature gradient and thermal conductivity measurements were taken using the standard needle probe with a string of four tensiometers emplaced in the sediments over a depth interval of 3.0–4.8 m below the lake bottom. They reported difficulties with penetration of the probe through the bottom layers, which contained a hard gypsum crust. They also reported on thermal instabilities of the bottom layer. Therefore, of a total of 25 heat flow measurements made in the lake, only 5 were considered valid.

On the other hand, Levitte et al. (1984) measured a much lower heat flux at a distance of 10 km, at the southern coast of the Sea of Galilee. They determined an average heat flow of 36.5 mW/m^2, with a range of 34.0 to 39.3 mW/m^2, over a depth interval of 2250–3470 m in a 4.2-km-deep borehole (Zemah-1). Thermal conductivity measurements were taken on both core samples and drill cuttings. The downhole temperature survey was conducted several months after completion of drilling operation, using a thermistor probe to obtain a continuous temperature log.

Most surprising are the significantly elevated geothermal anomalies detected outside the graben, at its shoulders (Fig. 2b). At the graben's western margin, at the Kinneret-6 well, a geothermal gradient of 48 °C/km was measured

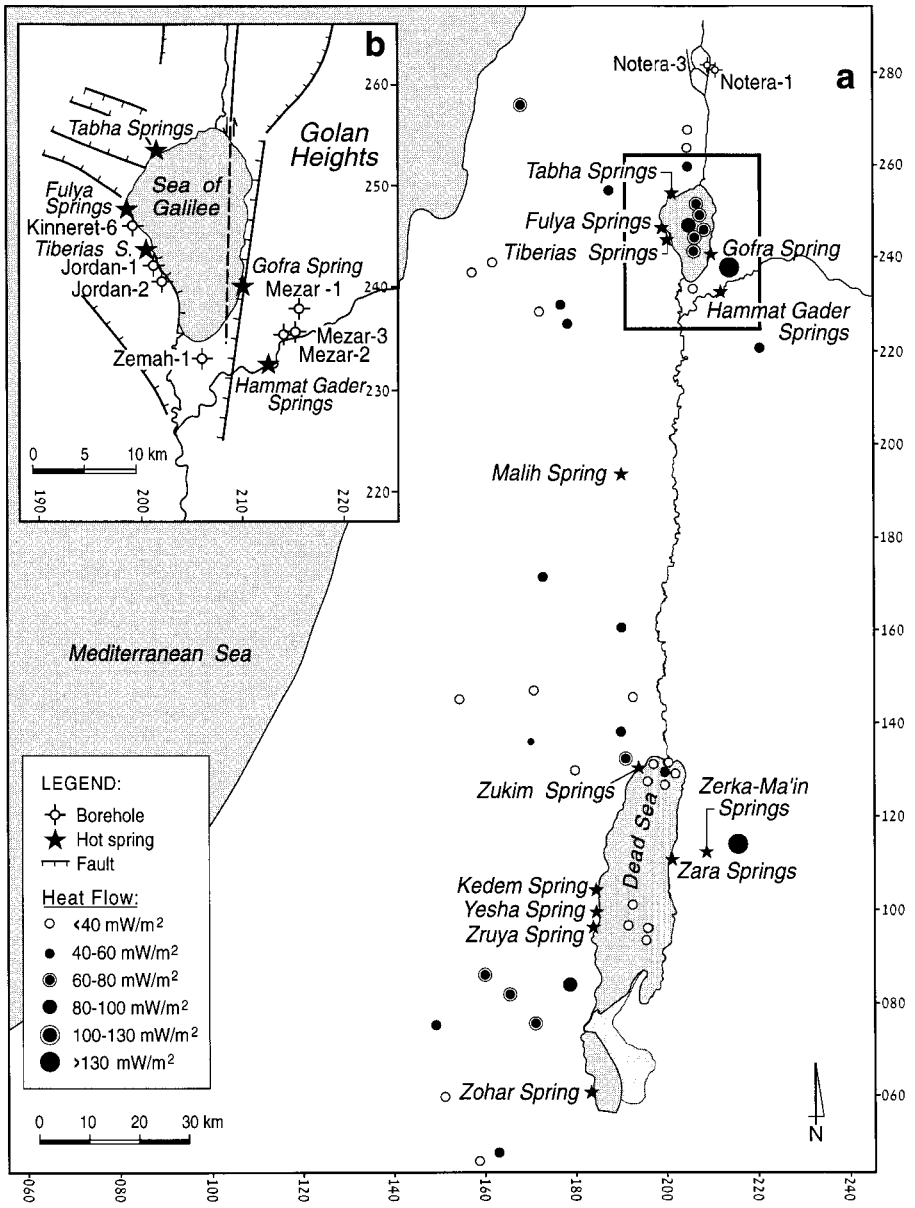

Figure 2. Heat flow maps of (a) hot springs along the rift (Table 1), wells in which heat fluxes were determined, and the line of the geologic cross section (Fig. 4); and (b) the vicinity of the Sea of Galilee, including boreholes where geothermal gradients were calculated (Fig. 3). Heat-flow data are based on Eckstein and Simmons (1978), Ben-Avraham et al. (1978), and Galanis et al. (1986).

(Fig. 3). The hot springs of Tiberias, Fulya, and Tabha, which have water temperatures of as much as 64 °C, emerge at the lake's western coast (Mazor et al., 1980). On the other side of the graben, in the 3 wells of Mezar, located 6–8 km east of the graben margin, geothermal gradients of 46 °C/km were measured (Fig. 3). It is evident that the geothermal gradient at these wells is about two to three times higher than that measured in Zemah-1 and other surrounding wells, some of which are shown in Figure 3 (Levitte and Olshina, 1985). The thermal conductivities of formations found in the Mezar wells were estimated by Mercado (1981) to be 2.9 W/m/°C. Thus, the heat flux is estimated to be 135 mW/m^2.

Eckstein and Maurath (1995) argued that at aquifer recharge zones, at higher elevations along the mountain backbone in Israel, where cool meteoric waters percolate downward, lower heat-flow values of 33 mW/m^2 (with standard deviation of 13 mW/m^2) are found, whereas in discharge zones along the Dead Sea rift, where hot waters ascend from deep aquifers, a heat-flow value of 75 mW/m^2 (with a standard deviation of 23 mW/m^2) was calculated. Similarly, in several other studies it was suggested that the thermal anomaly detected at the lake's western margin results from the ascent of hot brines from deep aquifers (Goldshmidt et al., 1967; Mazor, 1968; Gvirtzman et al., 1996). The most tangible expressions of the rift's convective hydrothermal systems are the warm to hot springs emerging along the margins of the rift (Table 1, Fig. 2).

In any case, this hypothesis can only explain the heat anomalies detected at locations where local conduits allow upward ground-water flow, such as the faults near the Tiberias, Fulya, and Tabha springs; however, it cannot explain the heat anomaly detected at the Mezar wells and Hammat Gader springs, because they are located some 6–8 km east of the rift fault system. Furthermore, hot waters ascending from deep aquifers in this area are highly saline (Table 1) due to mixing with deep-seated brines. However, the waters of Mezar wells and Hammat Gader springs are fresh, emerging from shallow aquifers (Starinsky et al., 1979; Arad and Bein, 1986). We believe that the thermal anomaly observed at the eastern side of the Sea of Galilee may be explained by large-scale free convection cells of deep ground water.

HYDROGEOLOGIC SETTING

An east-west detailed geologic cross section, 5 km deep by 70 km long, was prepared (Fig. 4) that traverses through the Galilee Mountains, Sea of Galilee, and the Golan Heights (A–A′ in Fig. 1). A list of lithostratigraphic units is appended (Table 2) that range in age from Triassic to Quaternary. The cross section was prepared using subsurface data collected from 20 deep boreholes and from several hundred kilometers of seismic lines carried out during oil exploration in northern Israel. A map of the top Judea Group (Klang and Gvirtzman, 1987; and Oil Exploration Investments Ltd. unpublished reports) served as a reference structural surface, and isopach maps of various pre-Judea stratigraphic intervals were used to construct the cross section. Lateral facies changes were included, such as the transition within the Kurnub Group (units Klw and Kle), and wedgeouts, such as the Asher Volcanics (unit Jlav) and Rosh Pina Formation (unit Jmr). The asymmetry of the stratigraphic sequence on the eastern and western sides of the rift valley is related to the 105 km shift along the left-lateral transform (Garfunkel, 1981). The stratigraphy within the rift valley was based on data from Zemah-1 borehole (Marcus and Slager, 1985). We empha-

size that the integrated stratigraphic sequence is grouped and divided into various hydrostratigraphic units (Table 2; Fig. 4) according to their estimated hydraulic properties.

Mesozoic to Tertiary sedimentary rocks crop out in the highlands on both sides of the rift valley and constitute the main recharge area for the major aquifers. Ground-water discharge to the rift is from three regional aquifers: (1) the 600-m-thick, Cretaceous Judea Group (unit Kmj), of predominantly platform carbonates; (2) the 400-m-thick, Lower Cretaceous Kurnub Group (units Klw and Kle), of mainly continental sandstones; and (3) the 2500-m-thick, Jurassic Arad Group (units Jln, Jms, and Juzh), of mainly platform carbonates.

The subsiding rift valley is capped by a Miocene–Quaternary sequence that is at least 4 km thick (Fig. 4) and that consists of evaporites, alluvial deposits, basalt, and a few intrusions of gabbro (Marcus and Slager, 1985); these rocks are mainly aquitards. The ground-water systems on both sides of the rift became separated due to juxtaposition of aquifers on the flanks with aquitards across the faults in the rift valley. Ground-water systems at the two sides of the graben behave differently (Arad and Bein, 1986). On the western margin of the graben, some downfaulted blocks expose the Judea aquifer (unit Kmj; not seen in Fig. 4) along the margins of the Sea of Galilee, channeling the main discharge of the system. Because continuity between aquifer units exists through downfaulted blocks (units Kle, Kmj and Pb; Fig. 4), ground water from deep aquifers flows upward and emerges as springs. On the other hand, on the eastern margin of the graben, the low-permeability chalk, salt, and marl sediments (units KuE, Ps, Pds, Mt, and Qds; Fig. 4) prohibit significant discharge from the regional deep confined aquifers to the outlets.

HYDROGEOLOGIC MODELING

Large-scale hydrogeologic models provide a useful approach for studying the nature of fluid migration in sedimentary basins, especially where the complexities of heterogeneity, structure, and coupled thermal and chemical processes preclude analytical solutions (Garven, 1995). Assuming a continuum approach under steady-state conditions, conservation of fluid mass is defined by

$$\nabla \cdot (\rho_f q) = 0 \qquad (1)$$

where ρ_f is the fluid density, and q is the specific flux, which is defined by Darcy's law,

$$q = (k\rho_o g/\mu)(\nabla h + \rho_r \nabla z), \qquad (2)$$

where k is the intrinsic permeability tensor, ρ_o is a reference fluid density, μ is the dynamic viscosity, g is the acceleration due to gravity, h is the equivalent fresh-water hydraulic head, and z is elevation above datum. This equation defines the two driving forces: the hydraulic head gradient and a buoyancy term. The relative fluid density, ρ_r, is defined by

$$\rho_r = (\rho_r - \rho_o)/\rho_o. \qquad (3)$$

Conservation of thermal energy, including both conduction and convection processes, under steady-state conditions is defined by

$$\nabla \cdot (\lambda \nabla T) - \rho_f c_f q \cdot \nabla T = 0, \qquad (4)$$

where λ is the effective thermal conduction-dispersion tensor of the porous medium, T is temperature, and c_f is the specific heat capacity of the fluid. Steady-state regional flow of variable-density ground water is best simulated using the stream function $\Psi(x,z)$ representation of flow lines and equivalent fresh-water head (Bear, 1972).

The numerical code used here is OILGEN (Garven, 1989), which has been successfully applied previously to several sedimentary basins around the world (e.g., Person and Garven, 1992; Garven et al., 1993; Haszeldine and McKeown, 1995). This two-dimensional code uses the finite-element method to solve the steady-state fluid and heat flow. Computations were conducted on a Silicon Graphics Personal IRIS 4D/35 workstation.

A two-dimensional finite element grid (21 rows by 44 columns in Fig. 5a) was developed by digitizing the geologic cross section (Fig. 4) to describe the geometry of the hydrostratigraphic units. Formation properties such as permeability, porosity, thermal conductivity, and fluid salinity were assigned for each element (Fig. 5b and Table 3). Next, boundary conditions were defined for ground-water flow and heat transport. Many of these parameters and boundary conditions were based by necessity on generalized assumptions and simplifications; however, the sensitivity to changes in assigned values of some of these parameters were analyzed and are described below.

Boundary conditions for the region of flow (Fig. 5, a and b) were defined as follows. The water-table surface, which is routinely monitored at tens of wells (Israel Hydrological Survey, 1996), forms the upper boundary to the region of flow. In the Galilee, the water table reaches elevations of 40 m above mean sea level at the water divide. Westward and eastward water-table gradients are different, because the base level at the west is the Mediterranean Sea, and at the east is the Sea of Galilee, where surface elevation is –210 m (below sea level). At

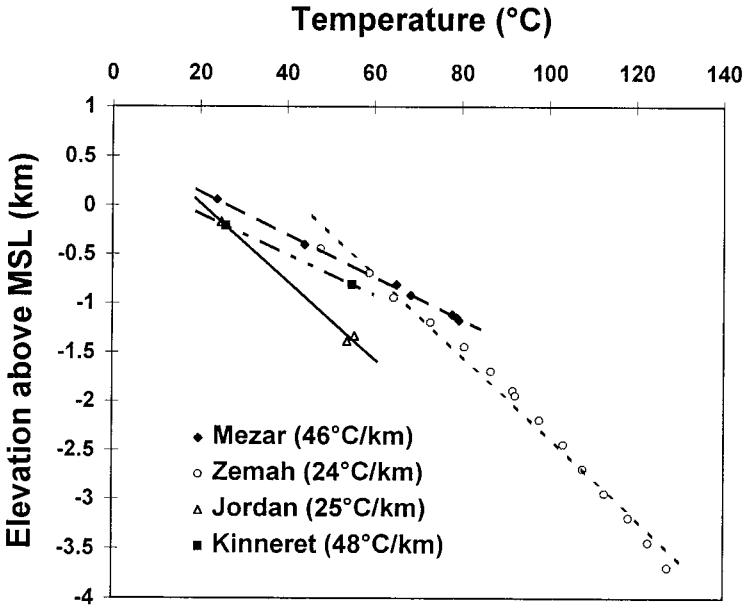

Figure 3. Temperature vs. depth (MSL—mean sea level) in deep wells around the Sea of Galilee, exhibiting the spatial variability of geothermal gradients. Number in parentheses, next to borehole names, indicate geothermal gradients calculated by linear regression. Because temperature at Kinneret-6 borehole was only measured at two depths, its significance is limited.

TABLE 1. HOT SPRINGS ALONG THE DEAD SEA RIFT VALLEY

Location	Name	West or east	Temp. (°C)	Chloride (mg/L)	References
Tabha	Hassartan	West	28	2800	Arad and Bein (1986), Mazor et al. (1980)
Tabha	Nur	West	29	1900	Arad and Bein (1986), Mazor et al. (1980)
Tabha	Druzi	West	26	1400	Arad and Bein (1986), Mazor et al. (1980)
Fulya	Russian Garden	West	27	800	Mazor et al. (1980)
Tiberias	Roman Spring	West	64	18000	Arad and Bein (1986), Mazor et al. (1980)
Gofra	Gofra Spring	East	31	2900	Arad and Bein (1986), Mazor et al. (1980)
Hammat Gader	Makle Spring	East	50	480	Arad and Bein (1986), Mazor et al. (1980)
Hammat Gader	Balsam Spring	East	42	330	Arad and Bein (1986), Mazor et al. (1980)
Hammat Gader	Reah Spring	East	37	240	Arad and Bein (1986), Mazor et al. (1980)
Hammat Gader	Sahina Spring	East	29	75	Arad and Bein (1986), Mazor et al. (1980)
Malih	Malih Spring	West	39	1200	Mimran (1969)
Zukim	#3	West	26	1080	Mazor et al. (1980)
Zukim	#4	West	27	7200	Mazor et al. (1980)
Zukim	#13	West	27	7650	Mazor et al. (1980)
Zerka-Main	#6	East	53	650	Rimawi and Salameh (1988)
Zerka-Main	#8	East	62	670	Rimawi and Salameh (1988)
Zerka-Main	#47	East	58	760	Rimawi and Salameh (1988)
Zerka-Main	#55	East	47	760	Rimawi and Salameh (1988)
Zara	#22	East	55	360	Rimawi and Salameh (1988)
Zara	#27	East	54	315	Rimawi and Salameh (1988)
Zara	#30	East	43	300	Rimawi and Salameh (1988)
Zara	#41	East	63	305	Rimawi and Salameh (1988)
Kedem	Kedem Spring	West	43	125000	Starinsky (1996, personal commun.)
Yesha	Yesha Spring	West	41	96300	Mazor et al. (1980)
Zruya	Zruya Spring	West	41	95000	Starinsky (1996, personal commun.)
Zohar	Zohar Spring	West	30	49900	Mazor et al. (1980)

Note: Springs are geographically ordered from north to south; their locations are shown in Figure 2.

TABLE 2. LITHOSTRATIGRAPHIC UNITS

Age	Symbol	Group	Formations	Lithology
Quaternary	Qds	Dead Sea	Lisan, "fill"	Marl
Pliocene	Pb	Dead Sea	Upper basalt	Basalt
Pliocene	Pds	Dead Sea	Unnamed	Marl
Pliocene	Psy	Saqiye	Yafo	Marl
Pliocene	Ps	Dead Sea	Sedom	Salt, gabbro
Miocene	Mt	Tiberias	Herods, Lower basalt	Marl, sand, basalt
Upper Cretaceous–Eocene	KuE	Shefela	Mount Scopus, Adulam, Maresha	Chalk, marl
Albian–Turonian	Kmj	Judea	Kamon, Dir Hana, Sakhnin, Bina	Dolomite, limestone, marl
Albian	Kaj	Judea	Zalmon, Yahini, Hidra, Asfuri, Rama	Marl, limestone
Lower Cretaceous	Kle	Kurnub	Hatira, Nebi Said, En el Assad	Sand, limestone, marl
Lower Cretaceous	Klw	Kurnub	Helez, Telamim, Yavne	Limestone, sand
Lower Cretaceous	Klt	Kurnub	Tayassir Volcanics	Basalt, pyroclasts
Upper Jurassic	Juzh	Arad	Zohar, Halutza	Limestone
Middle Jurassic	Jms	Arad	Sederot	Limestone, dolomite
Middle Jurassic	Jmr	Arad	Rosh Pina	Marl
Lower Jurassic	Jln	Arad	Nirim	Dolomite, limestone
Lower Jurassic	Jlav	Arad	Asher Volcanics	Basalt, pyroclasts

Note: Symbols correspond to those used in Figure 4.

the southern Golan Heights the regional water table is at about –40 m. For the steady-state modeling, we have assumed a constant water-table position; i.e., the rate of ground-water flow delivered to the water table from the surface is just the rate sufficient to maintain the water table in its equilibrium position. The lower boundary is located at 4–5 km depth, along the base of the sedimentary sequence studied, mostly at the base of the Jurassic layer. This surface is assumed to be impermeable to fluid flow. The two lateral boundaries are considered impermeable to fluid flow because they are assumed to occur where no horizontal hydraulic gradient exists. This assumption is reasonable because the western lateral boundary is located beneath the Mediterranean Sea shore, and the eastern one is located beneath the horizontal water table at the Golan Heights.

Thermal boundary conditions were defined as follows. A constant temperature of 20 °C, which is the mean annual air temperature, was assumed for the top surface. The lower boundary conditions, at 4–5 km depth, reflect the upward undisturbed heat flux, before it is redistributed by ground-water circulation. Therefore, steady geothermal fluxes of 60 mW/m^2 beneath the Galilee Mountains and of 72 mW/m^2 beneath the Dead Sea rift valley (eastern 30 km of the cross section) were assumed. Insulated boundaries have been assumed at both sides of the cross section. The components of fluid flow and heat flow normal to the cross section are assumed to be negligible, thereby justifying the two-dimensional representation of the basin.

At the initial stage of the simulation, the steady-state hydraulic head distribution was computed by assuming there are no salinity or temperature gradients. Darcy velocities were then computed for each element in the mesh. The steady-state heat equation was solved next to find the temperature pattern. With the new values of pressure and temperature, and the specified salinity distribution, fluid densities and viscosities were calculated from the equations of state. These four steps were repeated until the iterations converge to a stable temperature solution.

SIMULATION RESULTS

Results include equivalent fresh-water hydraulic head distribution, fluid velocity field, stream function, and temperature distribution throughout the cross section (Figs. 5, c, d, e and f, respectively). The hydraulic head distribution within the rift valley (Fig. 5c) demonstrates an artesian ground-water system. Through the upper 500 m of sediments beneath the lake's floor, the hydraulic head increases considerably with depth, forming a steep gradient toward the lake. The actual ground-water leak through these sediments, however, is relatively small due to the low permeability of the sediments (mainly marls). The springs through which this system is partially discharged are located only where specific conduits, such as faults, permit relatively easy pathways. In general, regions with dense isohydraulic-head lines are actually aquicludes (and aquitards) and those with lower density of lines are aquifers. The distribution of ground-water velocity across the two-dimensional section (Fig. 5d) is directly related to the head distribution and the permeabilities of the various units (Darcy law). It exhibits higher velocities in aquifers, especially in the Judea and Kurnub ones, and slower velocities in aquitards. In the Galilee, the highest velocities are found at the uppermost horizons of the Judea aquifer, discharging waters to both sides, eastward into the rift valley and westward toward the Mediterranean Sea. The velocity distribution also exhibits the typical slow rates in deep aquifers, such as the Arad one. The stream function (Fig. 5e) is an alternative way to demonstrate the flow field by tracing actual flow lines. These lines are plotted so that a constant amount of 10 m^3/yr per meter width of cross section is discharged between each pair. Consequently, dense flow lines are found in aquifers with relatively high discharge rates, such as the Judea and Kurnub ones. Where no flow lines are plotted, such as at depths of 3–5 km beneath the western and eastern edges of the Galilee Mountains, negligible discharges are found. These flow lines best present the free convection cells, one in the Kurnub and upper Arad aquifers, and a second

in the lower Arad aquifer (which are partially separated from each other by a thin aquitard). The distribution of temperatures (Fig. 5f) is directly related to the convective ground-water systems, as is explained in the following.

On the basis of these results, two types of basin-scale ground-water convection, and therefore of heat transfer, are suggested on both sides of the rift valley. The first is a simple forced convection which takes place at the western side of the valley (Fig. 5, d and e). Rainwater recharges at the Galilee Mountains, flows vertically to the shallow Judea aquifer and partially to the deep Kurnub and Arad aquifers (2–3 km deep) where it is heated, and discharges at the lake's western margin, creating the hot springs (Fig. 5f). The springs are actually a mixture of fresh and salty sources emerging from these aquifers (Goldshmidt et al., 1967). The fresh component drains laterally from the shallow Judea aquifer, and much of the saline component emerges as hot brines from the deeper Kurnub and Arad aquifers. The model predicts that average linear ground-water velocities at the Judea, Kurnub, and Arad aquifers approach 40, 5, and 0.8 m/yr, respectively (Fig. 5d), depending on the elevation of the ground-water table at the Galilee Mountains, and the hydraulic parameters of each of the hydrostratigraphic units (especially permeability and anisotropy). The total amounts of discharges per meter width of cross section are 750, 150, and 20 m^3/yr for the Judea, Kurnub, and Arad aquifers, respectively (Fig. 5e). A detailed discussion on the effect of changes in water table elevation on discharge rates was given by Gvirtzman et al. (1996).

A second ground-water flow mechanism exists at the eastern side of the valley; it is free convection, driven by buoyancy forces. Two thermally driven convection cells, 6–10 km in size, that flow counterclockwise (on the east-west section) are proposed for the confined, 3-km-thick, Cretaceous–Jurassic aquifers beneath the southern Golan Heights (Fig. 5e). The increasing temperature with depth creates physically unstable conditions, in which cold, high-density ground water lies above hot, low-density ground water. The model calculates that because the aquifer is thick enough and permeable enough (Fig. 5b), the common heat flux induces buoyancy forces to overturn the density inversion. Flow rates in these convection cells approach 1.0 m/yr in the Kurnub aquifer and 0.1 m/yr in the Arad aquifer (Fig. 5d), depending on the thickness of the aquifer, ground-water salinity gradient, permeability values, and anisotropy. This value fits with the common range of flow rate estimated for deep ground-water convection cells in hydrothermal systems (Evans and Nunn, 1989). The total amounts of heated-water vertical discharge per meter width of cross section are 40 and 20 m^3/yr for the Kurnub and Arad aquifers, respectively (Fig. 5e), resulting in a double regional geothermal gradient (Fig. 5f).

The counterclockwise flow direction within the free convection cells is explained as follows. The subsiding rift valley is filled by high-thermal-conductive evaporites. The lateral thermal conductivity difference between the evaporite beds in the rift (λ = 4 W/°C/m) and the surrounding carbonate rocks (λ = 3 W/°C/m) results in heat refraction, so that a larger amount of heat reaches the surface at the graben. Moreover, different vertical geothermal gradients are created at the sides of the graben's eastern fault. Therefore, at a given depth, a lateral temperature gradient is created toward the salt beds in the surrounding carbonate sediments, resulting in ground-water sinking adjacent to the salt and upwelling away from it; i.e., a counterclockwise motion (Fig. 5e). The model results are consistent with field observations (Starinsky et al., 1979; Bein and Feinstein, 1988): an elevated heat anomaly at Mezar wells and at the Hammat Gader springs, 6–8 km east of the graben margin. Note that a reversed flow circulation, with an upwelling along the salt flank, has sometimes been reported near salt diapirs (Jensenius and Munksgaard, 1989; Hanor, 1987). This pattern may exist under other conditions, such as higher contrast thermal conductivities, additional salinity gradients, or under isothermal conditions at the lower boundary (Evans and Nunn, 1989).

The influence of the right side boundary condition on the simulation results was tested by

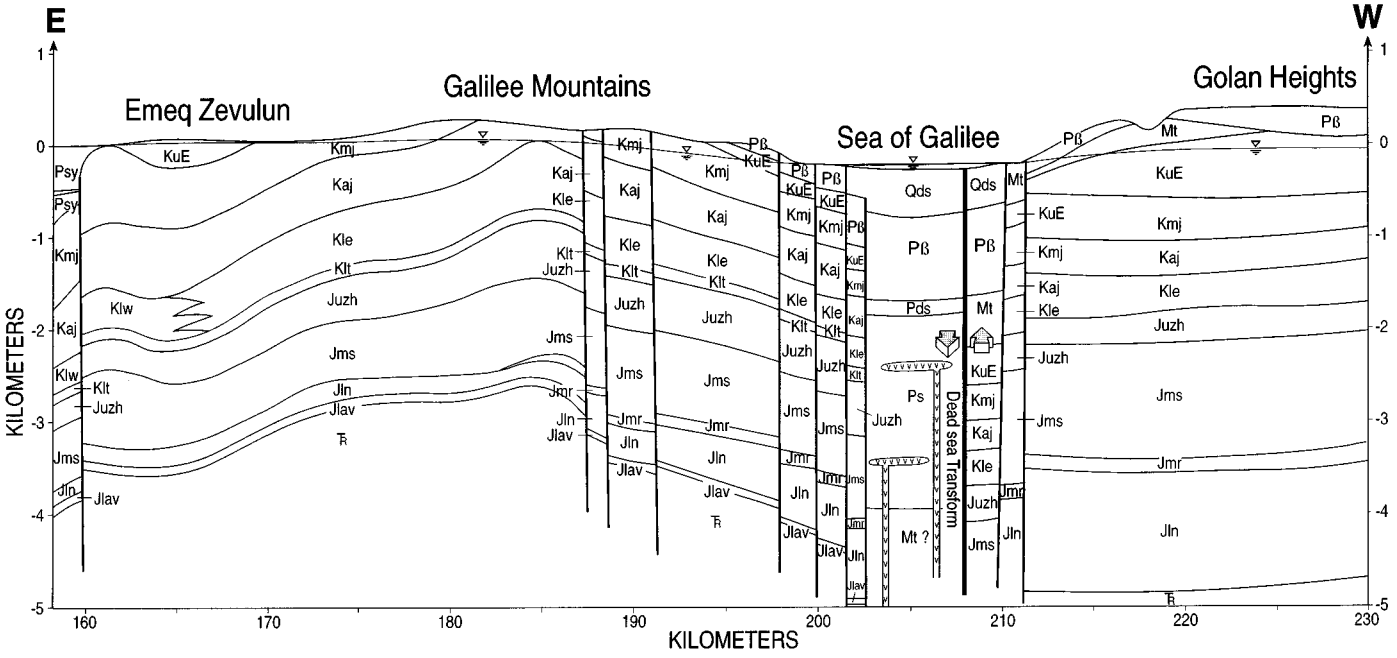

Figure 4. A geologic cross section through the Galilee Mountains, Sea of Galilee, and the Golan Heights (A–A′, Fig. 1). Symbols are listed in Table 2. Formations were grouped into hydrological units on the basis of their lithology and relative permeability. The thick line beneath the Sea of Galilee is the strike-slip transform and the nearby arrows give a sense of motion. Gabbro intrusions are drawn within the graben.

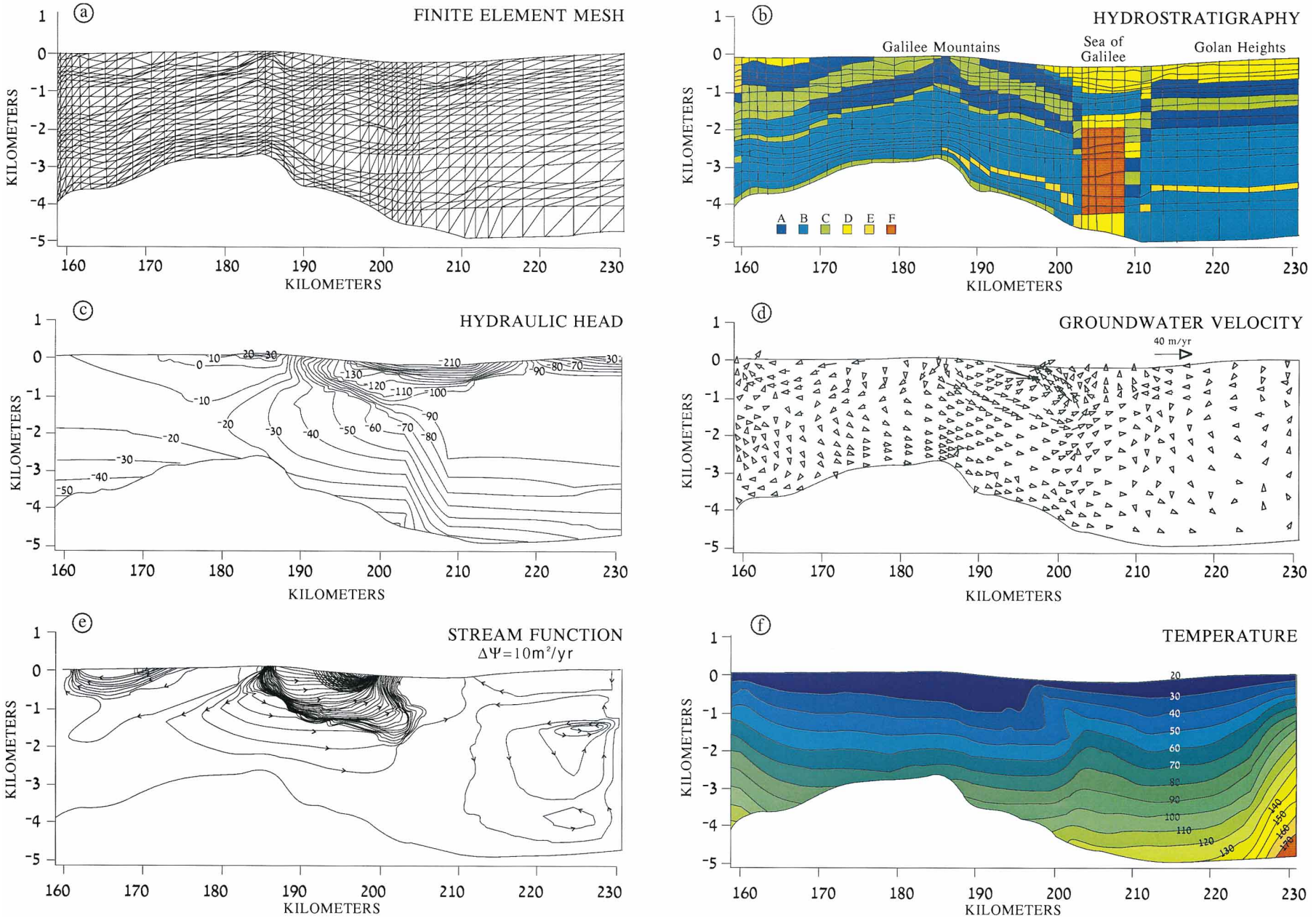

Figure 5. Results of the coupled variable-density ground-water flow and heat transfer model, carried out along the geologic cross section (Fig. 4), using the OILGEN (Garven, 1989) code and estimated rock properties (Table 3). Results include (a) finite element mesh; (b) hydrostratigraphic cross section, where units A–F are defined in Table 3; (c) equivalent fresh-water hydraulic head distribution; and (d) computed ground-water velocities (m/yr), where the vector length is linearly proportional to the flow rate. Note that high velocities are found in the two upper aquifers (unit A) emerging as springs at the Sea of Galilee western coast (Fulya Springs). (e) Stream function exhibiting the deep, buoyancy-driven, free convection cell beneath the Golan Heights, and the shallow, gravity-driven, convection beneath the Galilee Mountains. (f) Temperature distribution (degrees Celsius). Note that the heat anomaly at the Fulya Springs results from rising of deep hot ground water, and that beneath the Golan Heights (Mezar wells) results from the free convection cell.

moving it 20 km out. Results indicated that the counterclockwise-flow free convection cells remain, but new convection cells with a clockwise flow direction are located eastward of the previous ones. The total effect of these convection-cell pairs is an upwelling of deep ground water at the center, and downwelling on both sides. This results in a similar geothermal anomaly beneath the Mezar wells and Hammat Gader springs, as was predicted previously.

Because precise values for many of the hydrological parameters are unknown, especially at a large-basin scale, the sensitivity of the modeling results was checked against variations in assigned parameters. Through these analyses, it was found that flow rates are particularly sensitive to uncertainties of regional permeability, but the flow patterns persist throughout the tested hydraulic conductivity range (10–500 m/yr for the Judea and Kurnub aquifers). However, in other cases a change in an assigned permeability has caused a significant change in flow pattern. For example, a reduction in hydraulic conductivity of the Arad aquifer to below a certain value (K_H = 1 m/yr, where K_H/K_V = 100; see Table 3) stops fluid circulation in the free convection cell, and no heat anomaly is formed, which is inconsistent with field observations (Fig. 2b).

The results shown in Figure 5 are derived from many simulations in which parameters were modified until the comparison between calculated and the actual measured recharge, discharge, and geothermal gradients seemed favorable (Table 3). The simulations estimate an average recharge of 100 mm/yr at the Galilee Mountains, a discharge of about 900 m^3/yr per meter width slice at the Fulya springs, and geothermal gradients of 20 and 45 °C/km at the Galilee and Golan Heights, respectively. All these calculated values are in good agreement with measured ones.

Table 3 provides a list of most favored values of properties for groups of hydrostratigraphic units. The assigned thermal conductivity values are in very good agreement with those reported in the literature (Eckstein and Simmons, 1978; Ben-Avraham et al., 1978), which range between 0.76 and 3.6 W/°C/m, depending on the specific lithology. Similarly, the assigned permeability values fit those reported in the literature (Mercado and Mero, 1984; Michelson, 1975; Nativ, 1987; Nativ and Menashe, 1991). The estimated hydraulic conductivity of the Judea-Kurnub aquifer, K_H = 200 m/yr, is slightly higher than previously reported. Through a detailed study, Bein (1967) reported permeabilities of 1.0–0.01 mD using core permeameter measurements, and hydraulic conductivity of 1 m/day using aquifer pump tests. Using drill stem tests in these formations, Nativ and Menashe (1991) reported permeabilities of 1–20 mD. However, the hydraulic conductivity of carbonate and sandstone aquifers at the basin-scale is commonly almost two orders of magnitude higher than the permeability measured in the laboratory on core plugs, or about one order of magnitude higher than permeability measured by a pumping test at the field (Garven, 1995). Garven argued that the hydraulic conductivity measured in the laboratory reflects primary porosity; when measured at a borehole it reflects the macroscale fracture sets; however, at the basin scale it should reflect karst systems and regional fracture networks.

TABLE 3. HYDROLOGIC PARAMETERS ASSIGNED TO THE HYDROSTRATIGRAPHIC UNITS

Unit:*	Aquifer		Aquitard		Aquiclude	
	A	B	C	D	E	F
Formations:†	Kle, Kmj	Jln, Jms, Juzh, Klw, Eav, Pβ	Jlav, Klt, Kaj, Mt	KuE, Kums, Pds, Qds	Jmr, Psy	Ps
K_H (m/yr)§	200	10	5	0.5	0.1	0.001
K_V (m/yr)§	2	0.1	0.05	0.005	0.01	0.0001
Porosity (%)	15	5	8	10	3	1
λ (W/°C/m)	3	3	3	3	2	4

*Corresponds to hydrostratigraphic units defined in Figure 5a.
†Corresponds to formations shown in Figure 4 and Table 2.
§K_H and K_V are hydraulic conductivities along horizontal and vertical directions, respectively.

DISCUSSION

In principle, variations in heat flow may result from several different reasons. Variations in the concentration of radioactive heat-producing elements can lead to some differences in heat flow, but no evidence exists at the Dead Sea rift valley to support this hypothesis. Moreover, this is not a likely explanation because there is no way that it would result in the observed variations in heat fluxes (at least 40 mW/m^2) near the Sea of Galilee. On the other hand, the subsiding Dead Sea rift valley is characterized by a rapid sedimentation rate, which results in a lower heat flow. In addition, the various rock types in the rift (salt, gabbro, and marl) have different thermal conductivity values. Consequently, appreciable heat refraction into more conductive rocks can cause slight lateral variations. These hypotheses can explain the slight variations observed within the Dead Sea rift valley. It seems unlikely, however, that these mechanisms could be of sufficient magnitude to explain the high heat anomalies at the western margin of the Sea of Galilee, and especially, those at the Mezar wells at the east. We argue that ground-water convection is the major mechanism that causes redistribution of the heat within the rift valley, as follows.

The hydrological systems on the sides of the Sea of Galilee exhibit two types of ground-water convection: (1) a forced convection due to gravity forces at the western side; and (2) a free convection induced by buoyancy forces at the eastern side. These ground-water convections profoundly redistribute heat throughout the rift valley basin. At the western side, cold rainwater percolates at the high elevations of the Galilee Mountains, and is diverted vertically and laterally to the east. As water percolates downward, its temperature increases as it absorbs heat that would otherwise warm the sediments, thereby decreasing the thermal gradient (Fig. 5f). Ground water preferentially follows the path of least resistance, mostly through the Judea, and partially through the Kurnub and Arad aquifers. The upward flow of heated water at the western margin of the rift valley leads to elevated temperatures of the surrounding rocks, thereby increasing the thermal gradient. Eventual discharge occurs mostly as saline hot springs at high-permeable conduits, and also underneath parts of the lake's floor where relatively permeable filling material exists. At the eastern side of the graben, ground water in the deep Kurnub and Arad aquifers has neither inputs nor outputs; it is a closed hydrological system where free convection cells take place. At the upwelling zone, heat is transferred vertically by both mechanisms, conduction and convection, heating the surrounding rocks. Rising warm ground water at one location and sinking cold ground water at another location, increase and decrease the temperature gradients, respectively (Fig. 5f). The aquitard unit covering the Kurnub aquifer simply serves as a heat conductor layer between the deep convecting cell and the shallow Judea aquifer. The waters emerging from the hot springs at Hammat Gader originate from the shallow Judea aquifer; those at the western side emerge from deeper aquifers.

These two different mechanisms are actually a direct result of the specific geologic configurations developed through continental rifting. On the western side, the aquifer is phreatic at some portions and downfaulted blocks form a continuum between several aquifer units, discharging waters from shallow and deep aquifers and creating an open system (Fig. 5f). On the

eastern side, the aquifer is deep and totally confined. It is separated from the graben by a single major fault. The impermeable graben fill blocks discharge from the aquifer, creating a closed system. Moreover, the 105 km shift along the Dead Sea transform creates asymmetry of the stratigraphic sequence, so that on the western side, the Judea aquifer is exposed at a few locations at the lake's margin, but on the eastern side it is buried to great depth.

The two different ground-water convection systems are also expressed by the salinity data. The Hammat Gader springs and the Mezar wells contain fresh, hot waters, in contrast to the springs and wells at the lake's western coast, which contain saline hot ones (Table 1; Arad and Bein, 1986). These observations fit the geologic configuration and the modeling results. At the western side, the hot brines ascend from the deep aquifers and mix with shallow fresh ground water. However, at the eastern side, only fresh waters from shallow aquifers emerge; their heat, originated through the free convection cells in deeper aquifers, is transported by conduction through the intermediate aquitard.

As an alternative, it was suggested that the southern Golan Heights heat anomaly (Mezar wells and Hammat Gader springs) should be attributed to the extensive Miocene–mid-Pleistocene volcanism and intrusions (Arad and Bein, 1986). This explanation is questionable because the heat anomaly is observed only at the southeastern edge of the volcanic province, and nowhere else (Fig. 1a). Moreover, any intrusions seem likely to have cooled, since the last eruption took place 0.7 million years ago (Mor and Steinitz, 1984). The coalification profile from the Notera-3 deep well in the Hula basin (Figs. 1 and 2) indicated a relatively high thermal gradient averaging 40 °C/km throughout the Neogene (Bein and Feinstein, 1988); however, in the Notera-1 well, 0.6 km away, the recent thermal gradient is 13 °C/km (calculated from data of Levitte and Olshina, 1985). This temporal difference is obviously the result of the cooling process that took place after the Miocene–mid-Pleistocene volcanism and intrusions. In principle we agree with Arad and Bein (1986), that a minor residue of this magmatic heat source may still exist, but we argue that it is not enough by itself to induce the geothermal gradient (46 °C/km) and heat flux (135 mW/m^2) observed at the southern Golan Heights. Because of that, we have assumed in the modeling exercise a heat flux of 60 mW/m^2 at the lower boundary condition, at 4–5 km beneath the Galilee Mountains (which is the typical basal heat flux in northern Israel), and only 20% higher heat flux (72 mW/m^2) within the rhomb-shaped graben of the Sea of Galilee.

SUMMARY AND CONCLUSIONS

Ambiguous geothermal fluxes were measured at the vicinity of the Sea of Galilee, located within the Dead Sea rift valley: 70–80 mW/m^2 at the central part of the lake, 36 mW/m^2 at the lake's southern coast (10 km apart), and about 135 mW/m^2 at the southern Golan Heights, 6–8 km east of graben margin. This study argues that these geothermal anomalies directly result from ground-water convection systems, which redistribute the heat. Using a detailed geologic cross section that traverses the entire sedimentary basin and applying the OILGEN numerical code for solving the coupled variable-density ground-water flow and conductive-convective heat transfer equations, the observed temperature gradients along the entire cross section were reproduced. On the basis of the numerical simulations, two different mechanisms of basin-scale ground-water convection are suggested for the two sides of the rift that could influence the transport of heat: (1) forced convection (gravity-driven flow) of hot brines from deeper aquifers to the land surface at the western side; and (2) large-scale free convection (buoyancy-driven flow) of deep ground water at the eastern side. The different heat fluxes within the rift valley are attributed to the different lithology and to the locations of specific conduits through which the hot ground waters ascend from deeper horizons.

This study demonstrates the value of using hydrogeological modeling as a basic tool for understanding hydrogeological and hydrothermal systems. The existence of free convection cells of deep ground water beneath the southern Golan Heights, which has never been suggested previously, is hypothesized on the basis of such modeling. Moreover, through this study we have gained insights into (1) the mechanisms that generate the significantly different geothermal gradients near the Sea of Galilee and (2) the processes that create hot springs with extremely different salinities on the eastern and western sides of the rift.

Absolute flow magnitudes cannot be proven, verified, or validated by such models (Konikow and Bredehoeft, 1992; Oreskes et al., 1994). This study is based on a few generalized assumptions and simplifications because there are only poorly constrained hydrologic data for this region. There is much uncertainty regarding the exact location of faults beneath the lake, thickness of formations, properties of various lithostratigraphic units, and the three-dimensional temperature distribution. Nevertheless, this study is the first attempt to construct a comprehensive regional model of ground-water flow and heat transport across the Dead Sea rift valley, and we argue that a better understanding of the ground-water system behavior has been already achieved through this regional modeling. In any case, further hydrological, geophysical and geochemical investigations are required in order to understand the behavior of the entire hydrogeological system.

ACKNOWLEDGMENTS

We are grateful to our colleagues, H. Blatt, Y. Kolodny, A. Starinsky, and S. Feinstein, for their insightful remarks. We also thank Y. Eckstein and T. McKenna for their constructive comments on the manuscript.

REFERENCES CITED

Anderson, R. N., Hobart, M. A., and Langseth, M. G., 1979, Geothermal convection through oceanic crust and sediments in the Indian Ocean: Science, v. 204, p. 828–832.

Arad, A., and Bein, A., 1986, Saline versus freshwater contribution to the thermal waters of the northern Jordan rift valley: Journal of Hydrology, v. 83, p. 49–66.

Bear, J., 1972, Dynamics of fluids in porous media: New York, Elsevier, 764 p.

Bein, A., 1967, Hydrogeology of the Cenomanian–Turonian formations at the central-eastern Galilee [Master's thesis]: Jerusalem, Israel, Hebrew University, 88 p.

Bein, A., and Feinstein, S., 1988, Late Cenozoic thermal gradients in Dead Sea transform system basins: Journal of Petroleum Geology, v. 11, p. 185–192.

Ben-Avraham, Z., Hanel, R., and Villinger, H., 1978, Heat flow through the Dead Sea rift: Marine Geology, v. 28, p. 253–267.

Bently, H. W., Phllips, F. M., Davis, S. N., Habermehl, M. A., and Airey, P. L., 1986, Chloride 36 dating of very old groundwater, 1. The Great Artesian Basin, Australia: Water Resources Research, v. 22, p. 1991–2001.

Bethke, C. M., and Marshak, S., 1990, Brine migrations across North America—The plate tectonics of groundwater: Annual Review of Earth and Planetary Sciences, v. 18, p. 287–315.

Bredehoeft, J. D., and Norton, D. L., 1990, Mass and energy transport in the deforming Earth's crust, *in* The role of fluids in crustal processes: Washington, D.C., National Academy Press, p. 27–41.

Deming, D., Sass, J. H., Lachenbruch, A.H., and De Rito, R. F., 1992, Heat flow and subsurface temperature as evidence for basin-scale ground-water flow, North Slope of Alaska: Geological Society of America Bulletin, v. 104, p. 528–542.

Eckstein, Y., 1976, The measurements and interpretation of terrestrial heat flow in Israel [Ph.D. thesis]: Jerusalem, Israel, Hebrew University, 170 p.

Eckstein, Y., and Maurath, G., 1995, Terrestrial heat flow density and geothermal regime in Israel, *in* Gupta, M. L., and Yamano, M., eds., Terrestrial heat flow and geothermal energy in Asia: New Delhi, India, and Oxford, United Kingdom, IBH Publishers, p. 1–21.

Eckstein, Y., and Simmons, G., 1978, Measurements and interpretation of terrestrial heat flow in Israel: Geothermics, v. 6, p. 117–142.

Erickson, A. J., and Simmons, G., 1969, Thermal measurements in the Red Sea hot brines pool, *in* Degens, E. T., and Ross, D. A. eds., Hot brines and recent heavy metal deposits in the Red Sea: Berlin, Germany, Springer, p. 114–121.

Erickson, A. J., Simmons, G., and Ryan, W. B. F., 1977, Review of heatflow data from the Mediterranean and Aegean Seas, *in* Biju-Duval, B., and Montadert, L. eds., Structural history of the Mediterranean basins: Paris, France, Editions Technip, p. 263–280.

Evans, D. G., and Nunn, J. A., 1989, Free thermohaline convection in sediments surrounding a salt column: Journal of Geophysical Research, v. 94B, p. 12413–12422.

Folkman, Y., 1980, Magnetic and gravity investigations of the

Dead Sea rift and the adjacent areas in northern Israel: Journal of Geophysics, v. 48, p. 34–39.
Galanis, Jr., S. P., Sass, J. H., Munroe, R. J., and Abu-Ajamieh, M., 1986, Heat flow at Zerka-Ma'in and Zara and a geothermal reconnaissance of Jordan: U.S. Geological Survey Open-File Report 86-631, 110 p.
Garfunkel, Z., 1981, Internal structure of the Dead Sea leaky transform (rift) in relation to plate kinematics: Tectonophysics, v. 80, p. 81–108.
Garven, G., 1989, A hydrogeologic model for the formation of the giant oil sands deposits of the Western Canada sedimentary basin: American Journal of Science, v. 289, p. 105–166.
Garven, G., 1995, Continental-scale groundwater flow and geologic processes: Annual Review of Earth and Planetary Sciences, v. 23, p. 89–117.
Garven, G., Ge, S., Person, M. A., and Sverjensky, D. A., 1993, Genesis of stratabound ore deposits in the midcontinent basins of North America, 1. The role of regional flow: American Journal of Science, v. 293, p. 497–568.
Goldshmidt, M. J., Arad, A., and Neev, D., 1967, The mechanism of the saline springs in the Lake Tiberias depression: Geological Survey Israel Bulletin, v. 45, p. 14.
Gvirtzman, H., Garven, G., and Gvirtzman, G., 1996, Hydrogeological modeling of the saline-hot springs at the Sea of Galilee, Israel: Water Resources Research, v. 33, p. 913–926.
Hanor, J. S., 1987, Kilometer-scale thermohaline overturn of pore fluid in the Louisiana Gulf Coast: Nature, v. 327, p. 501–503.
Haszeldine, R. S., and McKeown, C., 1995, A model approach to radioactive waste disposal at Sellafield: Terra Nova, v. 7, p. 87–95.
Israel Hydrological Survey, 1996, Utilization and status of Israel water resources until autumn 1995: Jerusalem, Israel, Water Commission, ISSN-0793-1093, 205 p. (in Hebrew).
Jensenius, J., and Munksgaard, N. C., 1989, Large scale hot water migration systems around salt diapirs in the Danish central trough and their impact on diagenesis of chalk reservoirs: Geochimica et Cosmochimica Acta, v. 53, p. 79–88.
Kashai, E. L., and Croker, P. F., 1987, Structural geometry and evolution of the Dead Sea–Jordan rift system as deduced from new subsurface data: Tectonophysics, v. 141, p. 33–60.
Klang, A., and Gvirtzman, G., 1987, Structural contour map of the top Judea or Talme Yafe surface, Western Galilee and Mt. Carmel, the coastal plain and the continental shelf: Israel, Oil Exploration (Investments) Ltd., scale: 1:50,000, 1 sheet.
Konikow, L. F., and Bredehoeft, J. D., 1992, Groundwater models cannot be validated: Advance Water Resources, v. 15, p. 75–83.
Levitte, D., and Olshina, A., 1985, Isotherm and geothermal gradient maps of Israel: Jerusalem, Geological Survey of Israel Report GSI/60/84, 94 p.
Levitte, D., Maurath, G., and Eckstein, Y., 1984, Terrestrial heat flow in a 3.5 km deep borehole in the Jordan–Dead Sea rift valley: Geological Society of America Abstracts with Programs, v. 16, p. 575.
Marcus, E., and Slager, J., 1985, The sedimentary-magmatic sequence of the Zemah 1 well (Jordan–Dead Sea rift, Israel) and its emplacement in time and space: Israel Journal of Earth Sciences, v. 34, p. 1–10.
Mazor, E., 1968, Compositional similarities between hot mineral springs in the Jordan and Suez rift valleys: Nature, v. 219, p. 477–478.
Mazor, E., Levitte, D., Truesdell, A. H., Healy, J., and Nissenbaum, A., 1980, Mixing models and ionic geothermometers applied to warm (up to 60°C) springs: Jordan rift valley, Israel: Journal of Hydrology, v. 45, p. 1–19.
McKenzie, D., 1978, Some remarks on the development of sedimentary basins: Earth and Planetary Science Letters, v. 40, p. 25–32.
Mercado, A., 1981, The Ein-Said borehole, estimations of thermal and hydraulic parameters and evaluation of discharge-head and temperature relationships: Tel Aviv, Israel, Tahal, Water Consulting for Israel Report 01/81/111, 30 p. (in Hebrew).
Mercado, A., and Mero, F., 1984, The saline inflows of Lake Kinneret—Follow up Report #1, Chemical and isotope data-base and initial identification of hydrochemical processes: Tel Aviv, Israel, Tahal, Water Consulting for Israel Report 01/84/48, 144 p. (in Hebrew).
Michelson, H., 1975, The possibility of pumping fresh-water from the Low Cretaceous sandstones and limestones at the Lower Galilee: Tel Aviv, Israel, Tahal, Water Consulting for Israel Report 01/75/59, 22 p. (in Hebrew).
Mimran, Y., 1969, The stratigraphy of the Lower Cretaceous of Wadi Malih: Israel Journal of Earth Sciences, v. 18, p. 166–167.
Mor, D., and Steinitz, G., 1984, K-Ar age of the basalts at Nahal Orvim: Jerusalem, Geological Survey of Israel Report GSI/37/84, 11 p.
Musgrove, M., and Banner, J. R., 1993, Regional groundwater mixing and the origin of the saline fluids, midcontinent, U.S.: Science, v. 259, p. 1877–1882.
Nativ, R., 1987, Permeability distribution of the Jurassic Arad Group in the Negev: Israel Journal of Earth Sciences, v. 36, p. 155–160.
Nativ, R., and Menashe, S., 1991, The deep aquifers in northern Israel: Jerusalem, Israel, Hebrew University, Final Report to the Water Commission, 63 p. (in Hebrew).
Norton, D., and Knight, J., 1977, Transport phenomena in hydrothermal systems: cooling plutons: American Journal of Science, v. 277, p. 937–981.
Oreskes, N., Shrader-Frechette, K., and Belitz, K., 1994, Verification, validation and confirmation of numerical models in the earth sciences: Science, v. 263, p. 641–646.
Person, M. A., and Garven, G., 1992, Hydrologic constraints on petroleum generation within continental rift basins: Theory and application to the Rhine Graben: American Association of Petroleum Geology Bulletin, v. 76, p. 468–488.
Person, M., Raffensperger, J. P., Ge, S., and Garven, G., 1996, Basin scale hydrologic modeling: Reviews of Geophysics, v. 34, p. 61–87.
Rimawi, O., and Salameh, E., 1988, Hydrochemistry and groundwater system of the Zerka Ma'in–Zara thermal field, Jordan: Journal of Hydrology, v. 98, p. 147–163.
Starinsky, A., Katz, A., and Levitte, D., 1979, Temperature-composition-depth relationship in rift valley hot springs, Hammat Gader, northern Israel: Chemical Geology, v. 27, p. 233–244.
Toth, J., 1978, Gravity-induced cross-formational flow of formation fluids, Red Earth region, Alberta, Canada: Analysis, patterns, evolution: Water Resources Research, v. 14, p. 805–843.
Wood, J. R., and Hewett, T. A., 1982, Fluid convection and mass transfer in porous sandstones—A theoretical model: Geochimica et Cosmochimica Acta, v. 46, p. 1707–1713.

MANUSCRIPT RECEIVED BY THE SOCIETY APRIL 4, 1996
REVISED MANUSCRIPT RECEIVED DECEMBER 3, 1996
MANUSCRIPT ACCEPTED JANUARY 24, 1997

Printed in U.S.A.